

Excitation of $L = 1$, $S = 0$ Giant Resonances in the (p,n) Reactions on ^{90}Zr , ^{120}Sn , ^{140}Ce and ^{208}Pb at $E_p = 41 \text{ MeV}$

著者	Nishihara S., Furukawa K., Kabasawa M., Nakagawa T., Orihara H., Maeda K., Miura K., Ohnuma H.
journal or publication title	CYRIC annual report
volume	1983
page range	29-34
year	1983
URL	http://hdl.handle.net/10097/49159

I. 8 Excitation of $\Delta L = 1$, $\Delta S = 0$ Giant Resonances in the (p,n) Reactions on ^{90}Zr , ^{120}Sn , ^{140}Ce and ^{208}Pb at $E_p = 41$ MeV

Nishihara S., Furukawa K., Kabasawa M., Nakagawa T., Orihara H.*, Maeda K.**,
Miura K.***, and Ohnuma H.****

Department of Physics, Faculty of Science, Tohoku University

Cyclotron and Radioisotope Center, Tohoku University*

College of General Education, Tohoku University**

Tohoku Institute of Technology***

Department of Physics, Tokyo Institute of Technology****

A broad peak was observed at an excitation energy about 10 MeV above the Gamow-Teller giant resonance (GTGR or GTR) in the $^{90}\text{Zr}(p,n)^{90}\text{Nb}$ reaction at $E_p = 120$ MeV.¹⁾ This peak was tentatively assigned as 1^- from its angular distribution shape. Such broad peaks have been observed also in other low-energy and intermediate-energy (p,n) reactions²⁻⁴⁾, although no angular distribution has been published at a low-energy. Furthermore there are discrepancies between the reported values of the excitation energies and widths of these peaks.

An interpretation of these data has been proposed by Osterfeld and his collaborators based on their RPA calculations.⁵⁾ Similar to the $\Delta L = 0$ transitions, where the $\Delta S = 0$ mode yields the isobaric analog states (IAS) and the $\Delta S = 1$ mode GTR, the $\Delta L = 1$ collective excitation contains two modes: the $\Delta S = 0$ mode (1^-) corresponding to the anti analog state of the E1 giant resonance in the parent nucleus, and the $\Delta S = 1$ mode corresponding to the 0^- , 1^- and 2^- states. A low-energy (p,n) reaction may excite the $\Delta L = 1$, $\Delta S = 0$ mode selectively which is masked at intermediate energies by the dominant $\Delta L = 1$, $\Delta S = 1$ excitations due to the strong energy dependence of the $V_{\sigma\tau}/V_\tau$ ratio.⁶⁾ Here $V_{\sigma\tau}$ and V_τ are spin flip and spin non-flip isospin-dependent interaction strengths, respectively.

In this letter we report angular distribution measurements of the broad peaks observed above GTR in the (p,n) reactions on ^{90}Zr , ^{120}Sn , ^{140}Ce and ^{208}Pb at $E_p = 41$ MeV. A comparison with DWBA calculations using the TDA wave functions shows that they are indeed $\Delta L = 1$ transitions mainly of $\Delta S = 0$ components.

The experiment was performed using a 41-MeV proton beam from the AVF cyclotron and the time-of-flight facilities⁷⁾ at the Cyclotron and Radioisotope Center, Tohoku University. All the targets were self-supporting metallic foils. Their thicknesses and enrichments were: ^{90}Zr (6.2 mg/cm², 97.7 %), ^{120}Sn (10.1 mg/cm², 98.4 %), ^{140}Ce (15.5 mg/cm², 88.5 %), and ^{208}Pb (20.7 mg/cm², 98.7 %). Overall time resolution was typically 0.9 ns. The errors in the absolute magnitude of the cross sections, including the uncertainties of the detector efficiency but not those from the background estimation, are ≤ 20 %.

Sample neutron spectra taken with a flight path of 18 m are shown in fig. 1(b) together with a peak fitting results. The energy resolution was 330 keV in the vicinity of IAS. Two bumps observed in the $^{140}\text{Ce}(p,n)$ spectrum and interpreted as GTR's are discussed in our previous work.⁸⁾ Figure 2 shows the angular distributions for IAS and GTR for ^{140}Pr , and for the broad peaks above GTR.

The curves in fig. 2 are DWBA calculations which will be discussed later. A reasonable account of the data has been obtained for both the angular distribution shapes and cross section magnitudes if we assume the observed broad peaks are due to incoherent sums over the $\Delta L = 1$ transitions predicted by the TDA calculations. The resonance parameters of the $\Delta L = 1$ peaks are listed in table 1, and compared with the previously reported results.¹⁻⁴⁾ A good agreement are seen for IAS and GTR in table 1. On the other hand, significant disagreements are seen between the low-energy and intermediate-energy data. The centroid excitation energies of the $\Delta L = 1$ resonances are about 2 MeV higher at low incident energies, and the widths smaller.

Self-consistent HF + TDA calculations have been performed to understand the properties of the $\Delta L = 1$ resonances we observed. We have simply assumed proton and neutron shell closure at $Z=50$ and $N=82$, respectively, with the additional eight protons occupying the $g_{7/2}$ orbit in the case of ^{140}Ce . Similar assumptions have been made for ^{90}Zr , ^{120}Sn and ^{208}Pb . The inclusion of RPA correlations does not affect the present results appreciably due to the Pauli blocking by excess neutrons. By employing the Skyrme type interaction SGII⁹⁾, we obtained the bound-state wave functions and single-particle energies from a Hartree-Fock calculation. Here, we used an oscillator parameter $\nu (= m\omega/\hbar) = 0.1926 \text{ fm}^{-2}$. Then we performed lp-lh TDA calculations with the same SGII interaction in the model space of two major shells. The location of IAS and GTR were well reproduced in the present calculation as reported in our previous report⁸⁾ for the case of the $^{140}\text{Ce}(p,n)^{140}\text{Pr}$ reaction.

The DWBA cross sections have been calculated with the code DWBA70¹⁰⁾, which includes knock-on exchange contributions, using the spectroscopic amplitudes obtained from present TDA calculation. The effective interaction used in the DWBA calculation is the M3Y-even interaction¹¹⁾, which is obtained by switching off the odd-state parts of the central M3Y interaction¹²⁾ and has been successfully used for analyses of low-energy (p,n) data^{8,11)}. Optical potential parameters of Carlson et al.¹³⁾ are used for protons and neutrons. The DWBA cross section of the $\Delta L = 1$ transition at $\theta = 3^\circ$ for the $^{140}\text{Ce}(p,n)^{140}\text{Pr}$ reaction is displayed in the upper half of fig. 3. The (p,n) differential cross sections are calculated for 10 transitions for $\Delta J^\pi = 0^-$, 28 transitions for $\Delta J^\pi = 1^-$ and 34 transitions for $\Delta J^\pi = 2^-$, and then integrated over 2-MeV bins. Comparing fig. 3(a) and fig. 3(b), we find that the broad peak in the (p,n) spectrum is mainly due to the $\Delta S = 0$ transition predicted at $E_x \approx 25.5 \text{ MeV}$, though the reason why the $\Delta S = 1$ transitions to 2^- states predicted by the present calculation are so small is not clear. The $\Delta L = 1$ resonance observed in

a lower excitation region at the intermediate-energy (p,n) work may, on the other hand, correspond to the transitions leading to the $\Delta S = 1$, 2^- states predicted around $E_x = 22$ MeV, since at higher energies $\Delta S = 1$ transitions are favored. Indeed, a large spin-flip probability ($S_{NN} = 0.58 \pm 0.05$) observed¹⁴⁾ for the region $15 \leq E_x \leq 25$ MeV in the $^{90}\text{Zr}(p,n)^{90}\text{Nb}$ reaction at $E_p = 160$ MeV is a strong indication of this excitation mechanism. Such an interpretation is in agreement with that given by Osterfeld et al.⁷⁾ We have obtained similar results for the $^{90}\text{Zr}(p,n)^{90}\text{Nb}$, $^{120}\text{Sn}(p,n)^{120}\text{Sb}$ and $^{208}\text{Pb}(p,n)^{208}\text{Bi}$ reactions. The calculated angular distributions of the summed cross sections, thus obtained only for the $\Delta S = 0$, $\Delta L = 1$ pieces, are compared with the data in fig. 2. Simultaneous fit has been obtained for the three transitions leading to IAS, GTGR and the $\Delta L = 1$ giant resonance ($\Delta L = 1$ GR) for each target with no scaling to optimize comparison. If we use the original M3Y interaction, the ratio $\sigma(\text{exp})/\sigma(\text{calc})$ is about 0.5 for GTR and 0.7 for $\Delta L = 1$, $\Delta S = 1$ states but 1.3 for IAS and 1.0 for $\Delta L = 1$, $\Delta S = 0$ states.

In conclusion, we have measured the angular distributions of the broad resonances about 10 MeV above GTR in the (p,n) reactions on ^{90}Zr , ^{120}Sn , ^{140}Ce and ^{208}Pb at $E_p = 41$ MeV. The TDA and DWBA calculations reproduce the experimental cross section magnitudes and angular distribution shapes, indicating that these resonances are mainly 1^- states excited through the $\Delta L = 1$, $\Delta S = 0$ mode. The $\Delta L = 1$, $\Delta S = 1$ strength distribution predicted by the TDA calculation is consistent with the intermediate-energy (p,n) data.

The authors are indebted to Prof. Josef Speth for his helpful discussions. They are also indebted to Dr. S. Adachi and Dr. Y. Okuhara for their help in the TDA calculation.

References

- 1) Bainum D. E. et al., Phys. Rev. Lett. 44 (1980) 1751.
- 2) Sterrenburg W. A. et al., Phys. Rev. Lett. 45 (1980) 1839.
- 3) Horen D. J. et al., Phys. Lett. 95B (1980) 27; 99B (1981) 383.
- 4) Gaarde C. et al., Nucl. Phys. A369 (1981) 258.
- 5) Osterfeld F. et al., Phys. Lett. 105B (1981) 257.
- 6) Petrovich, in: The (p,n) reaction and the nucleon-nucleon force, ed. Goodman C. D. et al., (Plenum New York, 1980) p. 115.
- 7) Orihara H. and Murakami T., Nucl. Instr. Methods 188 (1981) 15.
- 8) Orihara H. et al., Phys. Lett. 118B (1982) 283.
- 9) Giai N. V. and Sagawa H., Phys. Lett. 106B (1981) 379.
- 10) Schaeffer R. and Raynal J., Saclay Report No. CEA-R4000 (1970), unpublished.
- 11) Ohnuma H. and Orihara H., Prog. Theor. Phys. 67 (1982) 353.
- 12) Bertsch B. et al., Nucl. Phys. A284 (1977) 399.
- 13) Carlson J. D., Zafiratos C. D. and Lind D. A., Nucl. Phys. A249 (1975) 29.
- 14) Taddeucci T. N. et al., Phys. Rev. Lett. 52 (1984) 1960.

Table 1. Experimental results for the IAS, GTGR and $\Delta S = 0$, $\Delta L = 1$ giant resonances. Data at intermediate energies are also listed for comparison.

E_p (MeV)		41 ^{a)}	45 ^{b)}	120 ^{c)}	200 ^{d)}
Target	state	resonance parameter (MeV)			
⁹⁰ Zr	IAS	$E_x^{e)}$	5.107	5.107	5.1
		width	—	—	—
	GTGR	E_x	8.6	8.19	8.7
		width	4.2	3.8	4.4
	$\Delta L=1, GR$	E_x	20.0	19.7	17.9
		width	4.2	3.8	7.8
¹²⁰ Sn	IAS	E_x	10.238	10.238	
		width	—	—	
	GTGR	E_x	12.2	12.29	
		width	4.4	3.6	
	$\Delta L=1, GR$	E_x	22.2	22.0	
		width	5.0	3.6	
¹⁴⁰ Ce	IAS	E_x	11.037		
		width	—		
	GTGR	E_x	12.4		
		width	3.8		
	$\Delta L=1, GR$	E_x	22.1		
		width	4.4		
²⁰⁸ Pb	IAS	E_x	15.172	15.172	15.2
		width	—	—	—
	GTGR	E_x	15.4	15.49	15.6
		width	2.6	2.9	4.2
	$\Delta L=1, GR$	E_x	23.5	24.14	21.5
		width	2.9	2.9	10

a) Present work.

b) Ref. 2.

c) Ref. 1.

d) Ref. 4.

e) Excitation energy in the residual nucleus.

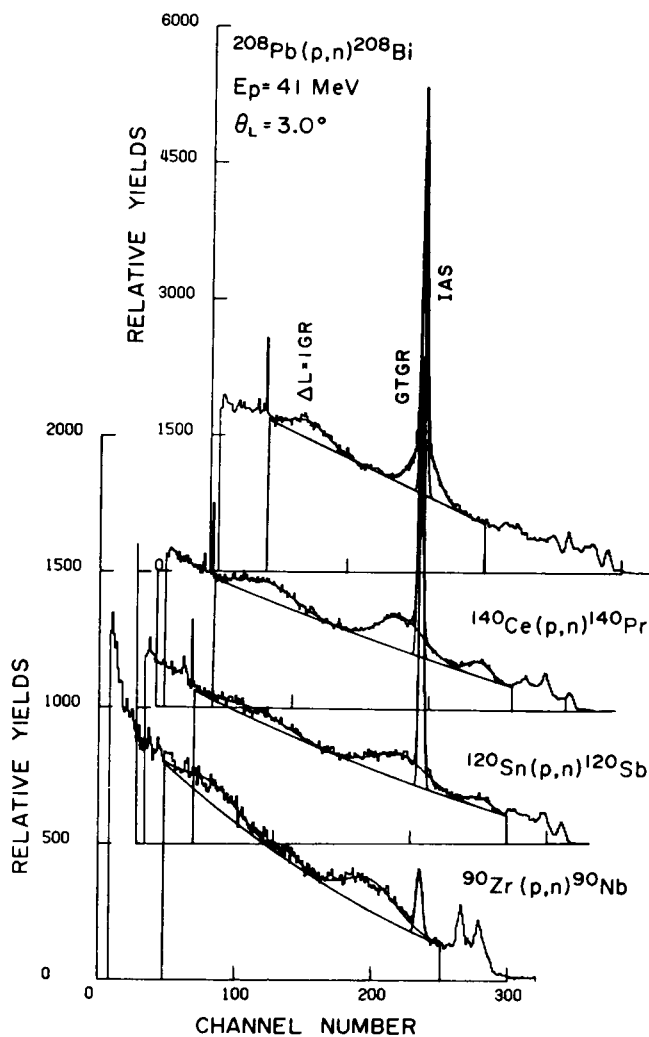


Fig. 1. Neutron energy spectrum for the (p,n) reactions on ^{90}Zn , ^{120}Sn , ^{140}Ce and ^{208}Pb at $\theta_{\text{lab.}} = 3.5^\circ$ measured with 41 MeV protons at a neutron flight path of 18 m. Solid curves are results of a peak fitting analysis. The abscissas are corrected for Coulomb displacement energies. The baselines for ^{120}Sn , ^{140}Ce and ^{208}Pb are shifted for display purposes.

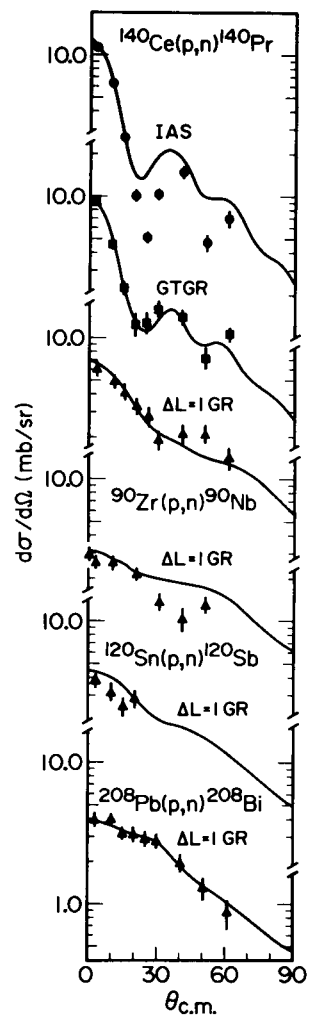


Fig. 2. Differential cross sections for the peaks corresponding to the 11.037 (IAS), 12.4 (GTGR) and 22.1 MeV in ^{140}Pr . Also shown are differential cross sections for neutrons leading to the broad resonances in ^{90}Nb , ^{120}Sb and ^{208}Bi at $E_x = 20.0$, 22.2 and 23.5 MeV, respectively. The curves are DWBA predictions described in the text.

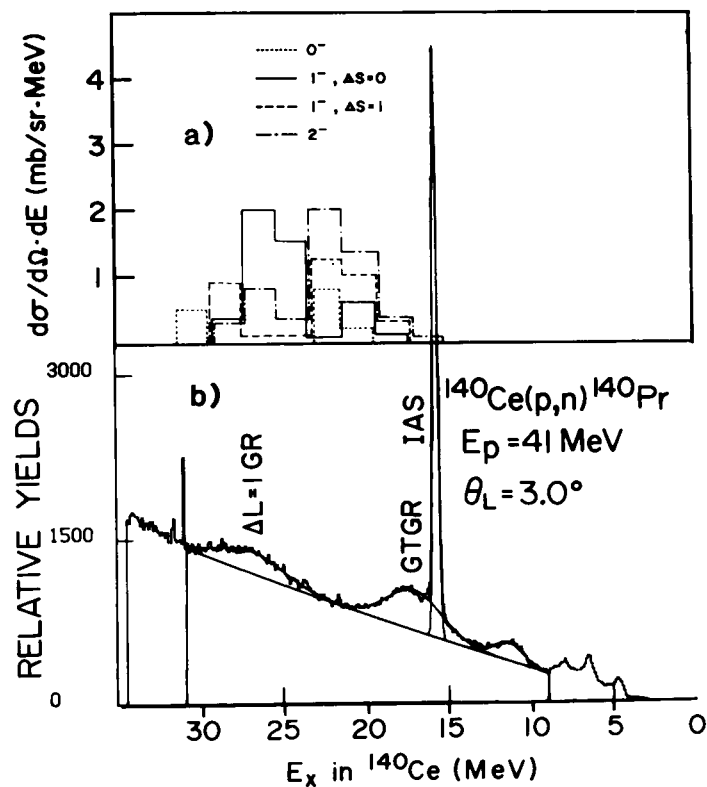


Fig. 3. The theoretical neutron energy spectra, obtained from the DWBA calculations for four $\Delta L = 1$ transitions, are compared with the experimental result for the $^{140}\text{Ce}(p,n)^{140}\text{Pr}$ reaction at $\theta_{\text{lab}} = 3^\circ$. The excitation energies are measured with respect to the ground state of ^{140}Ce E_x [(in ^{140}Pr) = E_x (in ^{140}Ce) + $Q(p,n)$].